

Kinetic Analysis of Non-isothermal Transformation of Zeolite 4A into Low-carnegieite

Cleo Kosanović,^{a,*} Boris Subotić,^a Alenka Ristić,^b and Lavoslav Sekovanić^c

^aRudjer Bošković Institute, Bijenička c. 54, 10000 Zagreb, Croatia

^bNational Institute of Chemistry, Hajdrihova 19, 1000 Ljubljana, Slovenia

^cGeotechnical Faculty, Hallerova 7, 42000 Varaždin, Croatia

RECEIVED AUGUST 19, 2003; REVISED OCTOBER 22, 2003; ACCEPTED OCTOBER 28, 2003

Kinetics of the non-isothermal transformation of zeolite 4A to low-carnegieite was investigated by the X-ray diffraction method. Changes in the fractions of zeolite 4A, amorphous aluminosilicate and low-carnegieite during zeolite 4A heating at three different heating rates ($0.0833\text{ }^{\circ}\text{ s}^{-1}$, $0.1667\text{ }^{\circ}\text{ s}^{-1}$ and $0.333\text{ }^{\circ}\text{ s}^{-1}$) showed that amorphization of zeolite 4A and crystallization of low-carnegieite take place simultaneously. Kinetic analyses of amorphization and crystallization showed that the non-isothermal transformation took place by the same mechanism as the isothermal transformation, *i.e.*, amorphization of zeolite 4A proceeded by a random, diffusion-limited agglomeration of the short-range ordered aluminosilicate subunits formed by the thermally induced breaking of Si-O-Si and Si-O-Al bonds between different building units of zeolite framework. Crystallization of low-carnegieite occurred by homogeneous nucleation of low-carnegieite inside the matrix of amorphous aluminosilicate and was diffusion-controlled, with one-dimensional growth of the nuclei. Kinetics of non-isothermal processes was determined by the changes of the rate constants during heating and the apparent activation energies of amorphization and crystallization.

Key words

non-isothermal transformation
zeolite 4A
amorphous aluminosilicate
low carnegieite
kinetics
mechanism

INTRODUCTION

Due to their open framework, zeolites are metastable materials that can be transformed to non-zeolite crystalline aluminosilicates above a certain temperature.^{1–7} Since many of synthetic zeolites have a composition close to that of aluminosilicate-based ceramics, their thermal treatment may result in the formation of ceramic materials.¹ The first step of the thermal transformation of zeolites is formation of an amorphous aluminosilicate phase by destroying the zeolite structure.^{1,3,5–8} The formed amorphous aluminosilicate has the same chemical composi-

tion as the original crystalline precursor (zeolite).^{6,8} Further transformation pathways of the amorphous aluminosilicates depend on the type of zeolite, type of the cation and the transformation temperature.^{3,4,6,9–13}

In this way, zeolites seem to be promising precursors to aluminosilicate-based ceramics,^{1,3–5,7,14} they are readily synthesized with a narrow particle size distribution and can be obtained at low cost.¹ Hence, there is no doubt that an understanding of the mechanism and kinetics of transformation may be a significant factor for better control of the transformation process and product

* Author to whom correspondence should be addressed. (E-mail: cleo@rudjer.irb.hr)

properties, and thus for controlled production of zeolite-based ceramics.

For this reason, we have considered the mechanisms and kinetics of high-temperature solid-state transformations of zeolites, using the isothermal transformation of zeolite 4A into low-carnegieite as the model system.¹⁵ Kinetic analysis of isothermal amorphization of zeolite 4A has shown that the change (decrease) in the fraction, f_A , of zeolite 4A can be expressed as:¹⁵

$$\frac{df_A}{dt} = -G(a) \rho(a) K(a)_{\text{nh}} f_A [p K(a)_{\text{g}}]^n (t - \tau)^n = -K(a) f_A (t - \tau)^{3/2} \quad (1)$$

and hence,

$$f_A = \exp(-K_A t^m) = \exp(-K_A t^{5/2}) \quad (2)$$

where, $K(a)_{\text{nh}}$ is the rate constant of the »nucleation« of the amorphous phase (*i.e.*, formation of short-range ordered aluminosilicate subunits with the rate $dN_a/d\tau$ proportional to the fraction f_A of the untransformed zeolite 4A; $dN_a/d\tau = K(a)_{\text{nh}} f_A$),¹⁶ $K(a)_{\text{g}}$ is the rate constant of agglomeration of the short-range ordered aluminosilicate subunits (»growth« of amorphous agglomerates), $G(a)$ and $\rho(a)$ are the geometrical shape factor and density of the formed amorphous phase, crystallized solid phase, τ is the time at which the »nuclei« are formed and start »to grow«, t is the overall transformation time, $n = r/p$ ($r = 1, 2$ or 3 for one-, two- or three-dimensional growth, $p = 1$ for a linear, size independent growth, and $p = 2$ for a diffusion-limited growth)^{15,17–21}, $K_A = G(a)\rho(a)K(a)_{\text{nh}} [p K(a)_{\text{g}}]^n/p = G(a)\rho(a)K(a)_{\text{nh}} [2 K(a)_{\text{g}}]^{3/2}/2$, and $m = n + 1$.^{15,20–22} The values of $r = 3$, and $p = 2$ indicate that the thermally-induced amorphization of zeolite 4A occurs by a random three-dimensional, diffusion-limited agglomeration of the short-range ordered aluminosilicate subunits (»nuclei«) formed by thermally-induced breaking of Si-O-Si and Si-O-Al bonds of the zeolite framework.¹⁵

On the other hand, the rate, df_C/dt , of the crystallization of low-carnegieite from the amorphous aluminosilicate can be expressed as,

$$\frac{df_C}{dt} = G(C) \rho(C) K(C)_{\text{nh}} f_a [K(C)_{\text{g}}]^n (t - \tau)^n = -K_C f_a (t - \tau)^{1/2} \quad (3)$$

where, $K(C)_{\text{nh}}$ and $K(a)_{\text{g}}$ are the rate constants of homogeneous nucleation and crystal growth of low-carnegieite, $G(C)$ and $\rho(C)$ are the geometrical shape factor and density of the formed low-carnegieite crystals, f_C is the mass fraction of low-carnegieite formed up to the transformation time t , $K_C = G(C) \rho(C) K(C)_{\text{nh}} f_a [K(C)_{\text{g}}]^n$ and,

$$f_a = 1 - f_A - f_C \quad (4)$$

is the mass fraction of amorphous aluminosilicate present in the system at any transformation time t . The values of $r = 1$ and $p = 2$ ($n = 1/2$) in Eq. (3) indicate that crystallization of low-carnegieite from amorphous aluminosilicate takes place by homogeneous nucleation of low-carnegieite inside the matrix of amorphous aluminosilicate, followed by diffusion-controlled, one-dimensional growth of the nuclei (crystals).

Despite the simplicity of kinetic analyses of isothermal transformation processes,^{17,23–28} linear, non-isothermal heating is the common technique of high-temperature solid-state transformations.^{17,24,29–32} The advantage of this technique is a shorter transformation process compared to isothermal transformations, which is suitable for practical applications. Although the basic mechanism(s) of transformation are expected to be the same during both isothermal and non-isothermal transformations, the kinetics of the processes may be different due to constancy (during isothermal transformations; see Eqs. (1)–(3)) or inconstancy (during non-isothermal transformations) of the nucleation and growth rate constants.

Hence, taking into consideration the known mechanisms of the stepwise isothermal transformation of zeolite 4A into low-carnegieite,^{6,15,33–35} the objective of this work is a kinetic analysis of the non-isothermal transformation of zeolite 4A into low-carnegieite in order to find the relations between kinetic parameters characteristic of isothermal and non-isothermal conditions, and thus enable prediction and control of the pathways of the transformation processes.

EXPERIMENTAL

The starting material (zeolite 4A) was synthesized in our laboratory by the method described previously.³⁶ In order to transform the zeolite 4A precursor into amorphous aluminosilicate and low-carnegieite, respectively, the samples were heated at a constant rate ($5 \text{ }^\circ\text{C min}^{-1}$, $10 \text{ }^\circ\text{C min}^{-1}$ and $20 \text{ }^\circ\text{C min}^{-1}$) in a chamber furnace with controlled temperature (ELPH –2, Elektrosanitarij). At predetermined times that elapsed since the beginning of heating, the samples were taken from the furnace and quenched under tap water in order to stop the transformation process and prepare the samples for analyses.

All the samples were characterized by the powder X-ray diffractometry. The X-ray diffractograms of the powdered samples were taken using a Philips PW 1820 diffractometer with a vertical goniometer and Cu-K α graphite radiation.

The weight fractions, f_A , of zeolite 4A, f_a , of the amorphous aluminosilicate and, f_C , of low-carnegieite were calculated by three different methods; Hermans-Weidinger method,³⁷ external standard method and the mixing method,³⁸ using the integral value of the broad amorphous peak ($2\theta = 17\text{--}39^\circ$) and the corresponding sharp peaks of the crystalline phases. The first method was used to determine of the

weight fractions of the crystalline phases in two-phase systems while the other two methods were used to determine the weight fractions of different amorphous and crystalline phases in the multi-phase systems.

RESULTS AND DISCUSSION

Figure 1 shows the changes of the fractions: f_A of zeolite 4A (A), f_C of low-carnegieite (B) and f_a of amorphous aluminosilicate (C) during non-isothermal heating of zeolite 4A at the rates of $0.0833 \text{ }^\circ\text{C s}^{-1}$ (solid curves, \square), $0.1667 \text{ }^\circ\text{C s}^{-1}$ (dashed curves, \circ) and $0.333 \text{ }^\circ\text{C s}^{-1}$ (dotted curves, \triangle). The changes of the fractions f_A , f_C , and f_a shown in Figure 1 undoubtedly demonstrate that the transformation process takes place through the sequence: zeolite (4A) \rightarrow amorphous aluminosilicate \rightarrow secondary crystalline phase (low carnegieite), characteristic of most of the temperature induced transformations of zeolites.^{1,3,5-8} As expected, the induction times of both processes, namely, amorphization of zeolite 4A (Figure 1A) and crystallization of low-carnegieite (Figure 1B) decrease with increasing the heating rate $\beta = dT/dt$ (T is temperature). Changes in the fractions of both crystalline phases (zeolite 4A, low-carnegieite) can be described by the sigmoidal curve, typical of most solid-state transformations.^{24,31,39} On the other hand, since crystallization of low-carnegieite starts before the overall amount of zeolite 4A has been transformed into amorphous aluminosilicate,

the change in the fraction $f_a = 1 - f_A - f_C$ of the amorphous aluminosilicate (symbols in Figure 1C) may be described by a bell-shaped curve (curves in Figure 1C). The bell-shaped change of fraction f_a is an additional evidence that non-isothermal heating of zeolite 4A resulted in gradual transformation of zeolite 4A into amorphous aluminosilicate (Figure 1A) and simultaneous crystallization of low-carnegieite (Figure 1B) from the amorphous aluminosilicate formed. As expected, the peak time, $t(a)_p$ decreases and the corresponding peak temperature $T(a)_p$ of the f_a vs. t curves (Figure 1C) increases with increasing the heating rate, *i.e.*, $t(a)_p = 10379.61 \text{ s}$ and $T(a)_p = 1148.13 \text{ K}$ for $\beta = 0.0833 \text{ }^\circ\text{C s}^{-1}$, $t(a)_p = 5451.97 \text{ s}$ and $T(a)_p = 1191.82 \text{ K}$ for $\beta = 0.1667 \text{ }^\circ\text{C s}^{-1}$ and $t(a)_p = 2840.04 \text{ s}$ and $T(a)_p = 1229.84 \text{ K}$ for $\beta = 0.333 \text{ }^\circ\text{C s}^{-1}$.

Numerical values of the rate constant K and reaction power $m = 1 + n$, relevant for isothermal transformations [see Eqs. (1)–(3) may be simply determined from $\ln(-\ln f_x)$ vs. $\ln t$ plot (for $df_x/dt < 0$, *e.g.*, $f_x = f_A$; see Figure 1A), or $\ln[-\ln(1-f)]$ vs. $\ln t$ plot (for $df_x/dt > 0$, *e.g.*, $f_x = f_C$; see Figure 1B), respectively. On the other hand, although it is realistic to assume that the value of m is not temperature dependent, the value of the rate constant K changes during a non-isothermal transformation in accordance with the Arrhenius law,²⁰ *i.e.*:

$$K(T) = K^\circ \exp(-E_a/RT) \quad (5)$$

where $K(T)$ is the value of the rate constant at appropriate temperature T , R is the gas constant, and a linear change (increase) of the transformation temperature T can be expressed as:

$$T = T_0 + \beta t \quad (6)$$

Then, a combination of Eqs. (1), (5) and (6) gives:

$$df_A/dt = -K(a)^\circ \exp[-E(a)_a/RT_0 + \beta t] f_A (t - \tau)^n \quad (7)$$

On the same principle, the combination of Eqs. (3), (5) and (6) gives:

$$df_C/dt = K(C)^\circ \exp(-E(C)_a/RT_0 + \beta t) f_a (t - \tau)^n \quad (8)$$

where, $K(a)^\circ$ and $K(C)^\circ$ are the apparent frequency factors in the Arrhenius equation, $E(a)_a$ and $E(C)_a$ are the apparent activation energies of the thermally induced amorphization of zeolite 4A and crystallization of low-carnegieite, $T_0 = 283 \text{ K}$ is the starting temperature of the transformation process and t is the time elapsed from the beginning of heating. Since analytical solution of Eqs. (7) and (8) cannot be expressed as a linear function of $f(t)$, which makes it impossible to determine K and m by the mentioned method.¹⁸⁻²⁰ Kissinger developed a method for the determination of apparent activation energy of non-isothermal processes based on the relation:⁴⁰

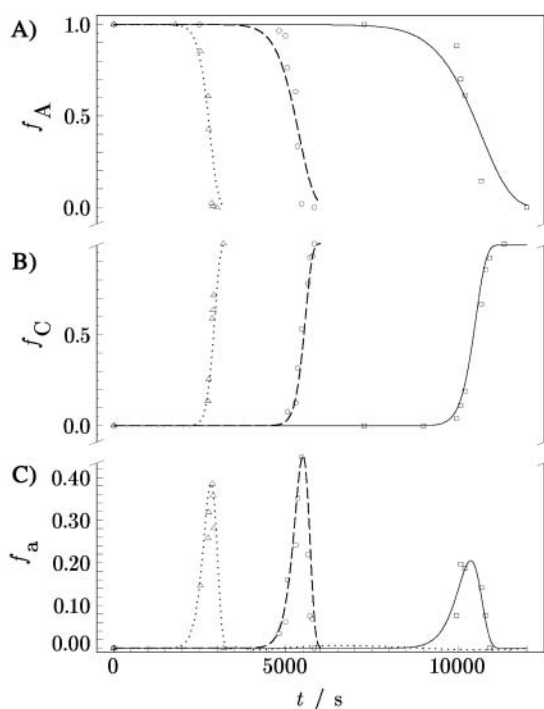


Figure 1. Changes of the fractions: (A) f_A of zeolite 4A, (B) f_C of low-carnegieite and (C) f_a of amorphous aluminosilicate during non-isothermal heating of zeolite 4A at the rates of $0.0833 \text{ }^\circ\text{C s}^{-1}$ (solid curves, \square), $0.1667 \text{ }^\circ\text{C s}^{-1}$ (dashed curves, \circ) and $0.333 \text{ }^\circ\text{C s}^{-1}$ (dotted curves, \triangle).

$$d [\ln (T_p)^2/\beta]/d (1/T_p) = E_a/R \quad (9)$$

and hence,

$$\ln [(T_p)^2/\beta] = k + E_a/(RT_p) \quad (10)$$

where, k is the integration constant and T_p is temperature of the maximum reaction (transformation) rate, *i.e.*, when $d^2f/dt^2 = 0$. Figures 2 and 3 show the linear relationships between $1/T_p$ and $\ln [(T_p)^2/\beta]$ relevant for the amorphization of zeolite 4A ($T_p = 1134.60$ K for $\beta = 0.0833$ ° s⁻¹, $T_p = 1168.60$ K for $\beta = 0.1667$ ° s⁻¹ and $T_p = 1201.7$ K for $\beta = 0.333$ ° s⁻¹) and crystallization of low carnegieite ($T_p = 1159.01$ K for $\beta = 0.0833$ ° s⁻¹, $T_p = 1193.70$ K for $\beta = 0.1667$ ° s⁻¹ and $T_p = 1234.9$ K for $\beta = 0.333$ ° s⁻¹). Hence, the apparent activation energies of the amorphization of zeolite 4A ($E(a)_a = 210.72$ kJ mol⁻¹) and crystallization of low-carnegieite ($E(C)_a = 197.6$ kJ mol⁻¹) were calculated as: $E_a = R/S$, where $S = E(a)_a/R$ is the slope of the $\ln [(T_p)^2/\beta]$ vs. $1/T_p$ straight line [see Eqs. (9) and (10) and Figures 2 and 3].

Using a multiple scan analysis technique,^{40,41} the values of m for non-isothermal transformations can be calculated by the relation:

$$m = -d[\ln(-\ln f_{x(T)})]/d(\ln \beta) \quad (11)$$

for $df_x/dt < 0$ (*e.g.*, $f_x = f_A$; see Figure 1A), or

$$m = -d\{\ln[-\ln(1 - f_{x(T)})]\}/d(\ln \beta) \quad (12)$$

for $df_x/dt > 0$ (*e.g.*, $f_x = f_C$; see Figure 1B)

where $f_{x(T)}$ is the mass fraction at the same temperature of a number of transformation kinetics under different heating rates.^{40,41} The values of $m = m(a) = 5/2$ (and thus $n(a) = m(a) - 1 = 3/2$) for amorphization of zeolite 4A and $m = m(C) = 3/2$ (and thus $n(C) = m(C) - 1 = 1/2$) for

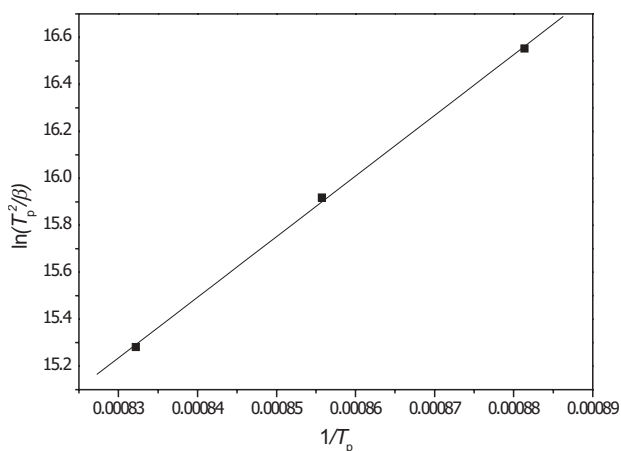


Figure 2. $\ln (T_p^2/\beta)$ versus $1/T_p$ plot (Kissinger plot) for the amorphization of zeolite 4A. β is the heating rate and T_p is the peak temperature.

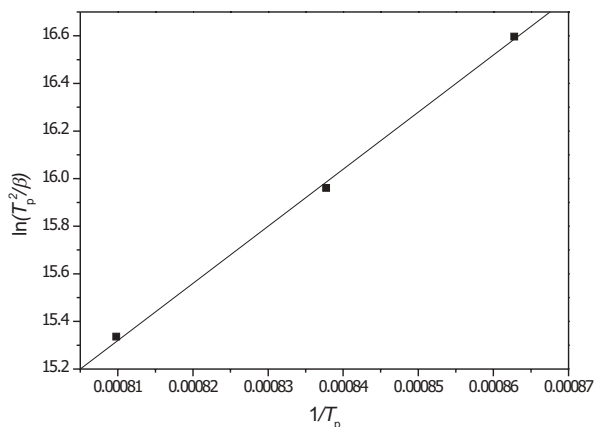


Figure 3. $\ln (T_p^2/\beta)$ versus $1/T_p$ plot (Kissinger plot) for crystallization of low-carnegieite. β is the heating rate and T_p is the peak temperature.

TABLE I. The values of the frequency factor $K(a)^\circ$ and exponent(s) n and m relevant for the amorphization of zeolite 4A at different heating rates β

$\beta / \text{° s}^{-1}$	$K(a)^\circ / \text{s}^{-1}$	n (m)
0.0833	4.1×10^{-2}	1.5 (2.5)
0.1667	3.4×10^{-1}	1.5 (2.5)
0.3333	1.0	1.5 (2.5)

crystallization of low-carnegieite, calculated by Eqs. (11) and (12), are the same as the corresponding values obtained by the analysis of isothermal transformation processes [see Eqs. (1)–(3)].¹⁵ This shows that the value of m and n , respectively, and thus the mechanisms of nucleation and growth rate depend neither on the temperature of transformation nor on the rate of heating. Now, using the known values of $E(a)_a$ (210.72 kJ mol⁻¹) and $n = n(a) = 3/2$, the changes in the fractions f_A of zeolite 4A during its heating at different rates were calculated (simulated) by an iterative numerical solution of differential Eq. (7) using the fourth-order Runge-Kutta method. Very good agreement between the measured changes of f_A (symbols in Figure 1A) and the calculated ones, using the values of $K(a)^\circ$ listed in Table I (curves in Figure 1A), shows that the differential Eq. (7) satisfactorily describes the mechanism (formation of short-range ordered aluminosilicate subunits and their diffusion-limited agglomeration) and the kinetics of non-isothermal amorphization of zeolite 4A. Since the values of $K(a)^\circ$ are a linear function of the heating rate β , *i.e.*, $K(a)^\circ = 3.8\beta - 0.28$, the kinetics of amorphization can be expressed as a function of the starting temperature T_0 and the heating rate β only, *i.e.*,

$$df_A/dt = -(3.8\beta - 0.28) \times \exp[-E(a)_a/R(T_0 + \beta t)] f_A (t - \tau)^{3/2} \quad (13)$$

On the other hand, because of simultaneous processes of the formation of amorphous aluminosilicate by amorphization of zeolite 4A and its instantaneous transformation into low-carnegieite, the change in f_a cannot be expressed as a simple function of f_C , *i.e.*, $f_a = 1 - f_C$,^{18–21} but it is a function of both f_A and f_C , respectively [see Eq. (4)]. For this reason, Eq. (8) contains two unknown variables ($K(C)^\circ$ and f_A), and thus it cannot be solved separately. However, since amorphization of zeolite 4A and crystallization of low-carnegieite are inter-dependent processes, the appropriate values of $K(C)^\circ$ may be determined by an iterative simultaneous numerical solution of the differential equations that describe simultaneous changes in f_A , f_a and f_C , *i.e.*,

$$df_A/dt = -K(a)^\circ \exp[-E(a)_a/R(T_0 + \beta t)] f_A (t - \tau)^{3/2} \quad (14)$$

$$df_C/dt = K(C)^\circ \times \exp[-E(C)_a/R(T_0 + \beta t)] (1 - f_A - f_C) (t - \tau)^{1/2} \quad (15)$$

$$df_a/dt = -(df_A/dt + df_C/dt) = K(a)^\circ \exp[-E(a)_a/R(T_0 + \beta t)] f_A (t - \tau)^{3/2} - K(C)^\circ \exp[-E(C)_a/R(T_0 + \beta t)] (1 - f_A - f_C) (t - \tau)^{1/2} \quad (16)$$

Changes in the values of f_A , f_C and f_a during the transformation at three different heating rates ($\beta = 0.0833^\circ \text{ s}^{-1}$, $0.1667^\circ \text{ s}^{-1}$ and $0.333^\circ \text{ s}^{-1}$) were calculated (simulated) by an iterative simultaneous solution of differential equations (14)–(16) [variation in the value of constant $K(C)^\circ$] using the fourth-order Runge-Kutta method and applying the known values of constant $K(a)^\circ$ (see Table II), $E(a)_a = 210.72 \text{ kJ mol}^{-1}$, $E(C)_a = 197.6 \text{ kJ mol}^{-1}$, $T^\circ = 283 \text{ K}$ and the initial conditions $(f_A)_0 = 1$, $(f_C)_0 = 0$ and $(f_a)_0 = 0$ [solutions of differential equations (14)–(16) for $t = 0$]. Figures 4–6 show that the agreement between the measured (symbols; ● for f_A and ○ for f_C) and calculated (solid curves for f_A and dashed curves for f_C) fractions is satisfactory or even very good for the applied values of constant $K(C)^\circ$ (see Table II). This undoubtedly shows that the mechanisms of non-isothermal amorphization of zeolite 4A ($n = 3/2$, $m = 5/2$) and crystallization of low carnegieite ($n = 1/2$, $m = 3/2$) are the same as the

TABLE II. The values of the frequency factor $K(C)^\circ$ and exponent(s) n and m relevant for the crystallization of low-carnegieite at different heating rates β

$\beta / ^\circ \text{ s}^{-1}$	$K(C)^\circ / \text{ s}^{-1}$	$n (m)$
0.0833	5.6×10^4	0.5 (1.5)
0.1667	1.0×10^3	0.5 (1.5)
0.3333	8.6×10^2	0.5 (1.5)

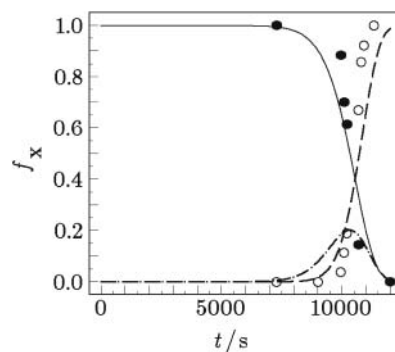


Figure 4. Correlation between fractions f_A of zeolite 4A (solid curve), f_a of amorphous aluminosilicate (dot-dashed curve) and f_C of low carnegieite (dashed curve) calculated by a simultaneous solution of Eqs. (14–16), and the values of f_A (●) and f_C (○) measured during non-isothermal heating of zeolite 4A at the heating rate $\beta = 0.0833^\circ \text{ s}^{-1}$.

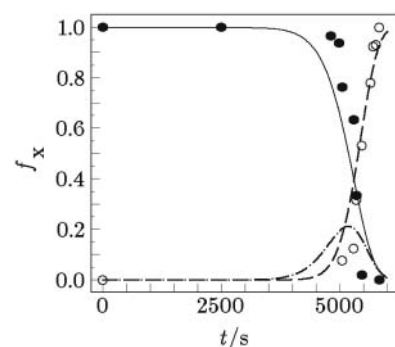


Figure 5. Correlation between fractions f_A of zeolite 4A (solid curve), f_a of amorphous aluminosilicate (dot-dashed curve) and f_C of low carnegieite (dashed curve) calculated by simultaneous solution of Eqs. (14–16), and the values of f_A (●) and f_C (○) measured during non-isothermal heating of zeolite 4A at the heating rate $\beta = 0.1667^\circ \text{ s}^{-1}$.

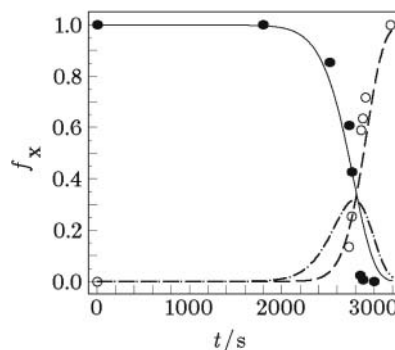


Figure 6. Correlation between fractions f_A of zeolite 4A (solid curve), f_a of amorphous aluminosilicate (dot-dashed curve) and f_C of low carnegieite (dashed curve) calculated by simultaneous solution of Eqs. (14–16), and the values of f_A (●) and f_C (○) measured during non-isothermal heating of zeolite 4A at the heating rate $\beta = 0.3333^\circ \text{ s}^{-1}$.

mechanisms of the corresponding isothermal process, and that the only difference is the change of the rate constants K_A and K_C [see Eqs. (1) and (3)] in accordance with the Arrhenius law [see Eqs. (5) and (6)] during heating. Hence, the change in fraction f_A of zeolite 4A can be expres-

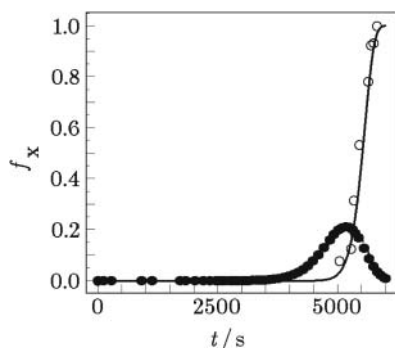


Figure 7. Correlation of fractions f_C of low-carnegieite calculated by Eq. (18) (solid curve) with the fractions of the low-carnegieite measured during non-isothermal heating of zeolite 4A at the heating rate $\beta = 0.1667 \text{ }^\circ\text{C s}^{-1}$ (o). The symbols (•) correspond to fractions f_o of the amorphous phase calculated by Eq. (17).

sed by Eq. (7) with $n = 3/2$, and the change in fraction f_C of low-carnegieite can be expressed by Eq. (8) with $n = 1/2$

Changes in fractions f_a of amorphous aluminosilicate calculated by the simultaneous solution of differential equations (14)–(16) (dash-dotted curves in Figures 4–6) differ a little from the measured fractions (symbols in Figure 1C). This was expected due to the (small) differences between the measured (symbols in Figures 4–6) and calculated (simulated) changes in fractions f_A and f_C (curves in Figures 4–6) and the calculation method, *i.e.*, $df_a/dt = -(df_A/dt + df_C/dt)$ [see Eq. (16)]. As shown previously,¹⁵ the bell-shaped f_a *vs.* t curves may be very well fitted by the empirical relation:

$$f_a = f_o q.k.t^{(q-1)}\exp(-k t^q) \quad (17)$$

where f_o , k and q are the appropriate constants. Figure 7 shows the fitting of the values of f_a calculated simultaneously with the solution of Eqs. (14)–(16), for $\beta = 0.1667 \text{ }^\circ\text{C s}^{-1}$ (•) by Eq. (17) with $f_o = 2 \times 10^2$, $k = 1.86088 \times 10^{-49}$ and $q = 13.096$ (dash-dotted curve). Taking into consideration the very good correlation between the measured (and/or simulated) values of f_a and the values of f_a calculated by Eq. (17), a combination of Eqs. (8) [or Eq. (15)] and (17) gives:

$$df_C/dt = K(C)^\circ \exp[-E(C)_a/RT_0 + \beta t] \times f_o q.k.t^{(q-1)} \exp(-k t^q) (t - \tau)^{1/2} \quad (18)$$

which describes the kinetics of non-isothermal crystallization of low-carnegieite from the amorphous aluminosilicate formed by non-isothermal amorphization of zeolite 4A. Figure 7 shows that the values of f_C calculated by numerical solution of Eq (18) with the same values of $K(C)^\circ = 1 \times 10^3$, $E(C)_a = 197.6 \text{ kJ mol}^{-1}$, $T_0 = 283 \text{ K}$ and $\beta = 0.1667 \text{ }^\circ\text{C s}^{-1}$, used in the simultaneous numerical solution of Eqs. (14)–(16), are in almost perfect agreement with the measured values of f_C . This confirms the finding that crystallization of low-carnegieite from the amorphous

aluminosilicate obtained by amorphization of zeolite 4A takes place by the proposed mechanism (homogeneous nucleation and diffusion-controlled, one-dimensional crystal growth, as indicated by the value of $n = 1/2$) and that the kinetics of crystallization can be satisfactorily described by Eq. (18).

CONCLUSIONS

Non-isothermal heating of zeolite 4A at linear rates of $0.0833 \text{ }^\circ\text{C s}^{-1}$, $0.1667 \text{ }^\circ\text{C s}^{-1}$ and $0.333 \text{ }^\circ\text{C s}^{-1}$ results in the pseudomorphic transformation of zeolite 4A into amorphous aluminosilicate and simultaneous crystallization of low-carnegieite. The presence of amorphous aluminosilicate and the bell-shaped change of its mass fraction f_a leads to the assumption that zeolite 4A cannot be transformed into low-carnegieite in a direct way (*e.g.*, by rotation and translation of the framework atoms) but that the first step of the thermal transformation of zeolite 4A is the formation of an amorphous aluminosilicate phase by destroying the zeolite structure. The formed amorphous aluminosilicate is then the precursor for nucleation and crystal growth of low-carnegieite.

The kinetic orders [values of n in Eqs. (7) and (8)], determined by a multiple scan analysis technique, of the non-isothermal transformation processes are the same as the kinetic orders previously determined for the corresponding isothermal transformations, *i.e.*, $n = 3/2$ for the amorphization of zeolite 4A and $n = 1/2$ for crystallization of low carnegieite. Hence, the mode of heating (isothermal or non-isothermal) does not affect the mechanism(s) of transformation. This means that in accordance with the Kolmogorov-Johnson-Mehl-Avrami-Evans (KJMAE) model of solid-state transformation processes, the non-isothermal amorphization of zeolite 4A takes place by a thermally-induced formation of short-range ordered aluminosilicate subunits and their diffusion-limited agglomeration into X-ray amorphous agglomerates, while non-isothermal crystallization of low-carnegieite takes place by homogeneous nucleation of low-carnegieite and diffusion-limited, one-dimensional growth of nuclei (crystals).

On the other hand, applying Kissinger's method, it was found that the rate constants $K(a)^\circ$ of the amorphization of zeolite 4A [Eq. (1)] and $K(C)^\circ$ of the crystallization of low-carnegieite [Eq. (3)] change with temperature in accordance with the Arrhenius law, and hence that the rates df_A/dt (differential change in the mass fraction f_A of zeolite 4A) and df_C/dt (differential change in the mass fraction f_C of low-carnegieite) can be expressed as:

$$df_A/dt = -K(a)^\circ \exp[-E(a)_a/RT_0 + \beta t] \times f_A (t - \tau)^{3/2} \quad [\text{Eq. (14)}]$$

$$df_C/dt = K(C)^\circ \exp[-E(C)_a/RT_0 + \beta t] \times (1 - f_A - f_C)(t - \tau)^{1/2} \quad [\text{Eq. (15)}]$$

where $E(a)_a = 210.7 \text{ kJ mol}^{-1}$ and $E(C)_a = 197.6 \text{ kJ mol}^{-1}$ are apparent activation energies of amorphization of zeolite 4A and crystallization of low-carnegieite, R is the gas constant, $T_0 = 283 \text{ K}$ is the starting temperature of the transformation process, $\beta = dT/dt$ is the rate of linear heating, $T = T_0 + \beta t$ is the temperature at the transformation time t , and $f_a = (1 - f_A - f_C)$ is the mass fraction of amorphous aluminosilicate at the transformation time t . The values of f_A calculated by an iterative numerical solution of Eq. (14) as well as the values of f_A and f_C calculated by a simultaneous iterative solution of Eqs. (14)–(16) are in very good agreement with the measured values of f_A and f_C , (Figures 4–6), thus indicating that the rate of non-isothermal amorphization of zeolite 4A can be satisfactorily described by Eq. (14), and that the rate of crystallization of low-carnegieite can be satisfactorily described by Eq. (15). This also confirms the assumption that only amorphous aluminosilicate is the precursor for crystallization of low-carnegieite.

It was shown that the change in the mass fraction f_a of amorphous aluminosilicate is a result of two simultaneous processes: its formation by amorphization of zeolite 4A and its spending during crystallization of low-carnegieite, *i.e.*, $df_a/dt = -(df_A/dt + df_C/dt)$ [see Eq. (16)], and thus, $f_a = (1 - f_A - f_C)$ [see Eq. (4)]. It was also shown that the bell-shaped f_a vs. t function can be very well fitted by the empirical relation, $f_a = f_0 q.k.t^{(q-1)} \exp(-k t^q)$ [see Eq. (17)], and thus, $df_C/dt = K(C)^\circ \exp[-E(C)_a/R(T_0 + \beta t)] f_0 q.k.t^{(q-1)} \exp(-k t^q) (t - \tau)^{1/2}$ [see Eq. (18)]. An excellent agreement between the measured values of f_C and the values of f_C calculated by the numerical solution of Eq. (18), which expresses the kinetics of crystallization of low-carnegieite from the amorphous phase (Figure 7), is an additional, very strong evidence that low-carnegieite may be formed only from the amorphous phase. Based on this finding, we are planning a more detailed study of the mechanism and kinetics of the temperature induced solid-state crystallization of low-carnegieite from precipitated Na-aluminosilicates.

Acknowledgements. – The authors thank the Ministry of Science of the Republic of Croatia and the Slovenian Ministry of Education, Science and Sport for financial support.

REFERENCES

1. M. A. Subramanian, D. R. Corbin, and U. Chowdhry, *Bull. Mater. Sci.* **16** (1993) 665–678.
2. M. Holioka, *J. At. Energ. Soc. Jpn.* **11** (1969) 406–411.
3. H. Mimura and T. Kanno, *Sci. Rep. RITU.* **29A** (1980) 102–111.
4. R. L. Bedard, R. W. Broach, and E. M. Flanigen, in: M. J. Hampden-Smith, W. G. Klemperer, and C. J. Brinker (Eds.), *Proc. Symp. Better Ceramics Through Chemistry V*, Materials Research Society, Pittsburgh, PA, 1992, pp. 581–587.
5. B. Hoghooghi, J. McKittrick, C. Butler, and P. Desch, *J. Non-Cryst. Solids* **170** (1994) 303–307.
6. C. Kosanović, B. Subotić, and I. Šmit, *Thermochim. Acta* **317** (1998) 25–37.
7. G. Dell'Agli, C. Ferone, M. C. Mascolo, and M. Pansini, *Solid State Ionics* **127** (2000) 309–317.
8. C. Kosanović, A. Čizmek, B. Subotić, I. Šmit, M. Stubičar, and A. Tonejc, *Zeolites* **15** (1995) 51–57.
9. L. Stock and I. Waclawska, *High Temp. Mater. Processes* **13** (1994) 181–201.
10. C. Kosanović and B. Subotić, *Microporous Mater.* **12** (1997) 261–266.
11. C. Kosanović, B. Subotić, I. Šmit, A. Čizmek, M. Stubičar, and A. Tonejc, *J. Mater. Sci.* **32** (1997) 73.
12. M. A. Subramanian, D. R. Corbin, and U. Chowdhry, *Adv. Ceram.* **26** (1989) 239–247.
13. C. Kosanović, B. Subotić, and A. Ristić, *Croat. Chem. Acta* **75** (2002) 783–792.
14. C. Hahn and K. Teuchert, *Ber. Dent. Keram. Ges.* **57** (1980) 208–214.
15. C. Kosanović, B. Subotić, and A. Ristić, (to be published elsewhere).
16. F. Von Goler and G. Sachs, *Z. Physik* **77** (1932) 281–287.
17. G. Ruitenbergh, E. Woldt, and A. K. Petford-Long, *Thermochim. Acta* **378** (2001) 97–105.
18. A. N. Kolmogorov, *Izv. Akad. Nauk. SSSR, Ser. Mater.* **3** (1937) 355–361.
19. W. A. Johnson and R. F. Mehl, *Trans. AIME.* **135** (1939) 416–424.
20. M. Avrami, *J. Phys. Chem.* **7** (1939) 1103–1112; **8** (1940) 212–224; **9** (1941) 177–184.
21. U. R. Evans, *Trans. Faraday Soc.* **41** (1945) 365–372.
22. L. Mandelkern, *Crystallization of polymers*, McGraw-Hill Book Company, New York, 1964, Chapter 8, pp. 215–290.
23. E. Tkalčec, S. Kurajica, and H. Ivanković, *Thermochim. Acta* **378** (2001) 135–144.
24. M. Bellotto, A. Gualtieri, G. Artioli, and S. M. Clark, *Phys. Chem. Minerals* **22** (1995) 207–214.
25. E. Woldt, *Metall. Mater. Trans. A.* **32A** (2001) 2465–2465.
26. X. Orhac, C. Fillet, R. Sempere, and J. Phalippou, *J. Non-Cryst. Solids* **291** (2001) 1–13.
27. J. Olivares, A. Rodríguez, J. Sangrador, T. Rodríguez, C. Ballesteros, and A. Kling, *Thin Solid Films* **337** (1999) 51–54.
28. S. P. Lin, K. Z. Fung, Y. M. Hon, and M. H. Hon, *J. Crystal Growth* **234** (2002) 176–183.
29. M. J. Starink, *J. Mater. Science* **36** (2001) 4433–4441.
30. M. J. Starink and A. M. Zahra, *Philosophic Magazine A*, **77**, No 1, (1998) 187–199.
31. A. Gualtieri, M. Bellotto, G. Artioli, and S. M. Clark, *Phys. Chem. Minerals* **22** (1995), 215–222.
32. A. Boutarfaia, M. Legouera, and M. Poulain, *J. Non-Crystalline Solids* **251(3)** (2001) 176–180.
33. Z. Pilter, S. Szabó, M. Hasznos-Nezdei, and E. Pallai-Varšányi, *Microporous Mesoporous Mater.* **40** (2000) 257–262.
34. T. Ohgushi, K. Ishimaru, and S. Komarneni, *J. Am. Ceram. Soc.* **84(2)** (2001) 321–327.

35. C. Kosanović and B. Subotić, 9th CIMTEC-World Ceramics Congress, *Ceramics: Getting into the 2000's-Part B*, (Ed. P. Vincenzini), Techna Srl., 1999.
36. R. W. Thompson and K. C. Franklin, *Verified Syntheses of Zeolitic Materials*, H. Robson (Ed.) Second Revised Edition 2001, p. 179.
37. P. H. Hermans and A. Weidinger, *Makromol. Chem.* **44/46** (1961) 24–48.
38. L. S. Zevin, L. L. Zavyalova, *Kolichestvenniy Rentgenographicheskiy Prazovij Analiz*, Nedra, Moscow, 1974, p. 37.
39. A. Gualtieri, P. Norby, G. Artioli, and J. Hanson, *Phys. Chem Minerals* **24** (1997) 191–199.
40. H. E. Kissinger, *Anal. Chem.* **29** (1957) 32–43.
41. P. L. López- Alemany, J. Vázquez, P. Villares, and R. Jiménez-Garay, *Thermochim. Acta* **374** (2001) 73–83.

SAŽETAK

Kinetička analiza neizotermne transformacije zeolita 4A u *low-carnegieite*

Cleo Kosanović, Boris Subotić, Alenka Ristić i Lavoslav Sekovanić

Kinetika neizotermne transformacije zeolita 4A u *low-carnegieite* istražena je metodom rentgenske difrakcije. Promjene u frakcijama zeolita 4A, amorfnoa alumosilikata i *low-carnegieite* tijekom grijanja zeolita 4A na tri različite brzine grijanja ($0,0833\text{ }^{\circ}\text{ s}^{-1}$, $0,1667\text{ }^{\circ}\text{ s}^{-1}$ i $0,333\text{ }^{\circ}\text{ s}^{-1}$) pokazale su da se amorfizacija zeolita 4A i kristalizacija *low-carnegieite* odvijaju istovremeno. Kinetičke analize amorfizacije i kristalizacije pokazale su da se neizotermna transformacija odvija istim mehanizmom kao i izotermna transformacija, tj. da se amorfizacija zeolita 4A odvija slučajnom difuzijski-ograničenom aglomeracijom podjedinica alumosilikata kratkog dometa koji su se stvorili termički induciranim razaranjem Si-O-Si i Si-O-Al veza između različitih jedinica građe zeolitne strukture. Kristalizacija *low-carnegieite* prouzrokovana je homogenom nukleacijom *low-carnegieite* unutar matrice amorfnoa alumosilikata te je kontrolirana difuzijom, s jednodimenzionalnim rastom jezgre. Kinetika neizotermnih procesa utvrđena je promjenama konstanti brzina tijekom grijanja i energijama aktivacije amorfizacije i kristalizacije.